Applied & Computational Mathematics
ISSN: 2168-9679

Dgheim, J Appl Computat Math 2015, 4:6
DOI: 10.4172/2168-9679.1000264

Research Article Open Access

Numerical Analysis of the Heat Transfer in Heterojunction Device for Optoelectronic Applications

Joseph Dgheim*

Laboratory of Applied Physics (LPA), Mechanical, Thermal and Renewable Energies Team (GMTER), Lebanese University, Lebanon

Abstract

Physical and numerical descriptions related to the heat transfer phenomenon inside the multilayer nanomaterial of thin film are determined. The mathematical model, of a multilayer of thin film of tin dioxide that deposits on a composite substrate of Silicon Dioxide/Silicon, is studied and solved by two numerical techniques, by taking into account the variability of the thermal conductivity. The two main interests in this study are the determination of the value of the applied maximum temperature on the multilayer nanomaterial, and the analysis, of the effect of the porosity medium that exists between certain layers, on the heat transfer. In plus, in order to determine our system physical parameters, the influence of the thickness of the thin deposit film is studied and the numerical model, which estimates these values in the heterojunction device, is analyzed.

Keywords: Nanomaterials; Heterojunction; Heat transfer; Tin dioxide; Multilayer

Introduction

With the continued reduction of dimensions of technological devices, the heat produced can be important, component failures can occur. According to NASA, 90% of failures are due to defects and thermal interconnects, according to the US Air Force, 55% of electronic failures are due to thermal effects [1]. The heat transfer control in these systems is a major challenge of miniaturization. Further reducing the size of the systems causes the decreased ability of materials to distribute heat when the scales are of the order of a nanometer or micrometer sometimes due to the spatial confinement effect in the nanostructures. Therefore, measurement of thermal parameters of thin films and heat transfer modeling in these systems are important from the theoretical point of view to understand the physical mechanisms underlying and from the point of view of the application to improve the design [2].

Heat transfer plays an important role in science and also affects the variation in the electrical, thermal and physical properties of materials. Heat transfer in semiconductor samples allows us to study the evolution of the temperature, taking account of the conduction and convection in the materials. The measurement in this area requires very sophisticated experiments because it requires considerable affinity. The temperature has an effect on the concentration of ionized impurity, the mobility and the electric conductivity of a semiconductor [3]. Some researchers [4] assume that the electrical conductivity is a constant at higher temperatures than room temperature. At high temperature, the particles are agitated with a thermally high kinetic energy. These particles cede its kinetic energy to neighboring particles having a low temperature for the entire system reaches thermal equilibrium.

The difference between a semiconductor and an insulator is that a semiconductor is low temperature insulation. It becomes conductive when its temperature becomes higher. Indeed, beyond a certain level of thermal motion,

the electrons of an intrinsic semiconductor gain sufficient energy to jump the band gap and move from the valence band to the conduction band. Thus, it exists, an electron pair and an occurrence of conduction by both electrons and holes [3]. At high temperatures, the intrinsic conductivity can be the major factor in the conductivity of a semiconductor. In an oxide insulator or semiconductor, the width of the band gap (energy gap, Eg), which by its magnitude, prevents thermally excited electrons to jump from the valence band to the conduction band. With a thermal agitation, the temperature rises and the heat transfer begins to settle. The fact that the conduction electrons carry the electrical and thermal loads, Weidman Franz [5] established a law linking the thermal conductivity to the electric one. The thermal conductivity dependent on the movement of charge carriers is called conductivity by electrons or holes. It depends on the concentration of charge carriers. In semiconductors, this quantity must greatly depend on the temperature.

Because of its connection to the mechanical and chemical stability of the layers, good adhesion to various substrates, stability under the action of aggressive fluids, its high conductivity, transparency in the visible spectral range, low cost, high sensitivity and rapid response, the nanocrystals of tin dioxide (SnO_2) is considered an attractive material for various technological applications include electronic and optoelectronic devices, electroluminescent displays, photocells, detectors, sensors and anti-reflection coatings [6-10]. In the hetero-structure $SnO_2/SiO_2/Si$, the interfacial layer (SiO_2) plays an important role in reducing the dark current, leading to the improvement of the circuit voltage in the cell. It is, in this framework, that this research will be established.

The first investigations on single crystals of SnO_2 are due to Jaruzelski [11]. He measured the optical absorption, and the electrical conductivity in the crystal. Jaruzelski analyzed the pattern of energy levels in single crystals SnO_2 with the photoelectric method. Morgan and Wright [12] studied the electrical conductivity in single crystals of SnO_2 doped with antimony. An idea that the gas sensor can be

***Corresponding author:** Joseph Dgheim, Laboratory of Applied Physics (LPA), Mechanical, Thermal and Renewable Energies Team (GMTER), Lebanese University, Lebanon, Tel: 9611612830; E-mail: jdgheim@ul.edu.lb

Received October 01, 2015; **Accepted** October 24, 2015; **Published** October 29, 2015

Citation: Dgheim J (2015) Numerical Analysis of the Heat Transfer in Heterojunction Device for Optoelectronic Applications. J Appl Computat Math 4: 264. doi:10.4172/2168-9679.1000264

developed using a metal oxide semiconductor used to detect toxic gases was developed using the sintering of SnO_2. These gas sensors have evolved according to the method of obtaining layers of tin dioxide [13].

Mathematical model

A mathematical model that describes the transfer of heat in heterojunction device is proposed. This model is based on the two dimensional heat transfer equation. It may present a roughness shape and heat resistance. The thermal conductivity of the material also has a great influence on the transfer process. Thermo-physical properties of the used materials are determined in order to thermally study the physical system that is formed by several materials in contact. Thus, the structural design of a modern sensor can be schematized by a physical model consisting of an insulating layer between two semiconductor layers. It is presented by the following Figure 1.

In this system, the heat transfer that develops in the heated tin dioxide layer having a thickness of 0.2 microns coupled with another layer of cold silicon, having a thickness of 1 micron, is studied numerically. A third layer of silicon dioxide, SiO_2 is considered between these two layers.

To complete the mathematical model, the relation that links the two thermal (λ) and electrical (σ) (conductivities given by Weidman Franz [5] is used:

$$\lambda = L\sigma T \text{ where } L = \pi^2 k^2 / \left(3e^2\right) = 2.44.10^{-8} (\mathrm{w}\,\Omega / \mathrm{K}^2) \quad (1)$$

The tin dioxide thermal conductivity, that is function of temperature, is given by this curve Figure 2.

Using the least squares method, correlation between the thermal conductivity and the temperature of the tin dioxide is given by the following Equation:

$$\lambda = -2.136 \times 10^{-4} \times T^2 + 0.078 \times T + 27.484 \quad (2)$$

In this case, silicon is a substrate followed by an insulating layer. Then, the silicon layer is not strongly influenced by the heating temperature. As a result, the thermal conductivity of the silicon is considered constant (149W/(mK)). In addition, the SiO_2 layer serving as an insulator, has a very low electrical conductivity. Then, its thermal conductivity is constant (1.4 W/(mK)). Finally, the mathematical model is represented in the following Figure 3.

To simplify the mathematical model, the following simplifying conditions are used: Heat transfer is carried out in a two-dimensional

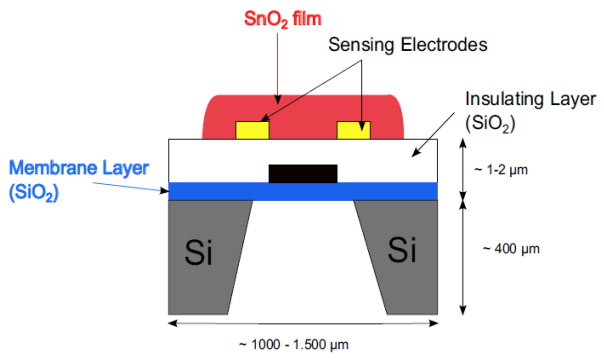

Figure 1: Structural design of a modern sensor.

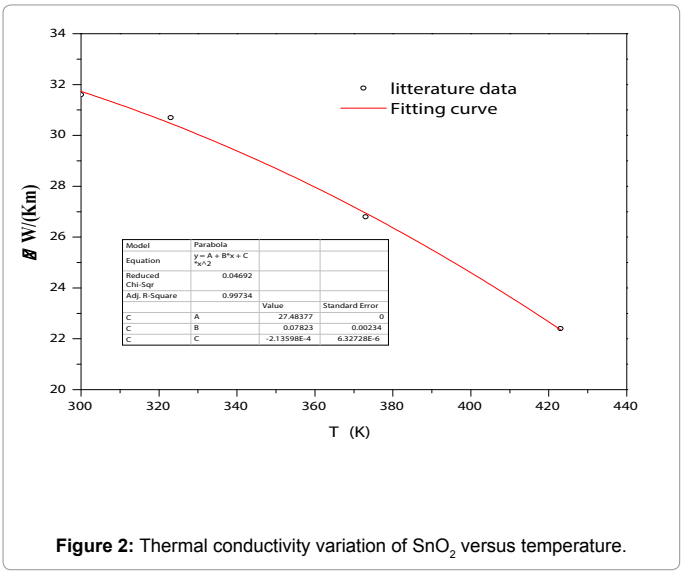

Figure 2: Thermal conductivity variation of SnO_2 versus temperature.

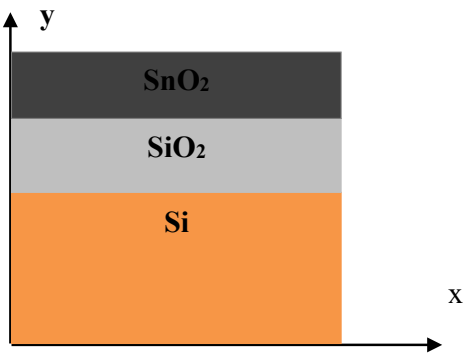

Figure 3: Mathematical model.

transient manner, the transfer occurs without heat generation and without chemical reaction, there is no generated heat flow, the pressure is the atmospheric one, the radiation effects are considered negligible. Using these simplifying conditions, the heat equation is the following:

$$\rho C_p \partial T / \partial t = \partial\left(\lambda \partial T / \partial x\right) / \partial x + \partial\left(\lambda \partial T / \partial y\right) / \partial y \quad (3)$$

With ρ is the density and C_p is the specific heat of the used materials.

Taking into account the variability of the thermal conductivity as a function of the temperature in the tin dioxide layer, the equation (3) becomes:

$$\begin{aligned}&\left(-4.272 \times 10^{-4} T + 0.078\right)\left(\partial T/\partial x\, \partial T/\partial x + \partial T/\partial y\, \partial T/\partial y\right) + \\ &\left(-2.136 \times 10^{-4} T^2 + 0.078T + 27.484\right)\left(\partial^2 T/\partial x^2 + \partial^2 T/\partial y^2\right) = \rho Cp\, \partial T/\partial t\end{aligned} \quad (4)$$

To complete the mathematical model, the simplified heat equation is linked to the initial and boundary conditions (Figure 4) as the following:

Initial conditions for $t<t_0$

For: $x=x_0$ to x_n and $y=y_0$ to y_n then $T=T_0=298.15$ K

Boundary conditions for $t>t_0$

For $x=x_0$ For $x=x_n$

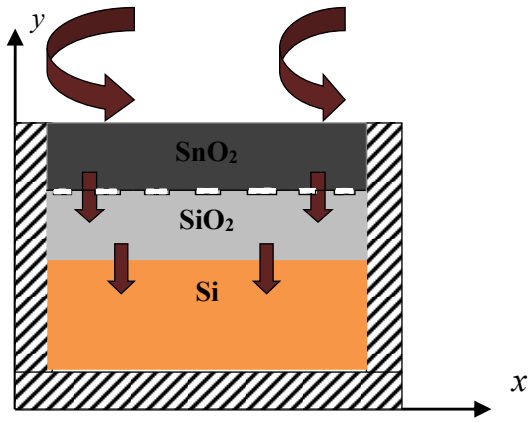

Figure 4: Boundary conditions of the SnO_2/Air/SiO_2/Si.

Q=0 (adiabatic system) $\Rightarrow \partial T/\partial x\big]_{x_0}$ =0 Q=0 (adiabatic system) $\Rightarrow \partial T/\partial x\big]_{x_n}$ =0

For $y=y_0$ For $y=y_n$ (5)

Q=0 (adiabatic system) $\Rightarrow \partial T/\partial y\big]_{y_0}$ =0 Q=hΔT

With Q is the heat quantity and h is the convective heat transfer coefficient.

Continuity at the interfaces:

At the SnO_2/air and air/SiO_2 interfaces, the continuity of the conduction and the convection is given by the following relationships:

$$\lambda_{SnO_2}\,\partial T/\partial y\big]_{SnO_2} = \lambda_{air}\,\partial T/\partial y\big]_{air} + h\left(T_a - T\right) \quad (6)$$

$$\lambda_{SiO_2}\,\partial T/\partial y\big]_{SiO_2} = \lambda_{air}\,\partial T/\partial y\big]_{air} + h\left(T_a - T\right) \quad (7)$$

Where, T_a is the ambient medium temperature.

At the interface Si/SiO_2, the continuity of the thermal conductivities is given by the following relationship:

$$\lambda_{Si}\,\partial T/\partial y\big]_{Si} = \lambda_{SiO_2}\,\partial T/\partial y\big]_{SiO_2} \quad (8)$$

At the interface of the two layers SiO_2 and SnO_2, the continuity of the thermal conductivities is given by the following relationship:

$$\lambda_{SiO_2}\,\partial T/\partial y\big]_{SiO_2} = \lambda_{SnO_2}\,\partial T/\partial y\big]_{SnO_2} \quad (9)$$

Numerical treatment

The equations of the mathematical model that describes the physical phenomenon are schemed by two numerical methods: the explicit finite difference method and the finite element method.

Scheming with the explicit finite difference method: The computational domain is divided into computing network nodes (iΔx, jΔy, nΔt). Δx and Δy, are the space steps, and Δt is the time step. The schemed form of the two-dimensional heat transfer equation with variable thermal conductivity in the case of tin dioxide is the following:

$$T_{(i,j)}^{n+1} = T_{(i,j)}^{n}\left[1 - A\boldsymbol{\lambda}_{(i,j)}^{n} - A\boldsymbol{\lambda}_{(i-1,j)}^{n} - B\boldsymbol{\lambda}_{(i,j)}^{n} - B\boldsymbol{\lambda}_{(i,j-1)}^{n}\right] + A\left[T_{(i+1,j)}^{n}\boldsymbol{\lambda}_{(i,j)}^{n} + \mathbf{T}_{(i-1,j)}^{n}\boldsymbol{\lambda}_{(i-1,j)}^{n}\right] + B[\mathbf{T}_{(i,j+1)}^{n}\boldsymbol{\lambda}_{(i,j)}^{n} + \mathbf{T}_{(i,j-1)}^{n}\boldsymbol{\lambda}_{(i,j-1)}^{n}] \quad (10)$$

With $A = \Delta t/\left(\rho C_p \Delta x^2\right) B = \Delta t/\left(\rho C_p \Delta y^2\right)$

And $\lambda_{(i,j)}^{n} = -2.136\times10^{-4}\times T^{2n} + 0.078\times T^{n} + 27.484$

Similarly, the initial and boundary conditions (5-9) are schemed in the following manner:

Initial conditions:

T(1:nx,1:nny,1)=298.15 K

Boundary conditions:

T (1:nx,nny,1:m)=673.15 K; (Hot face)

T(1,1:nny,1:m)=T(2,1:nny,1:m); (Adiabatic face)

T(nx,1:nny,1:m)=T(nx-1,1:nny,1:m); (Adiabatic face)

T(1:nx,1,1:m)=T(1:nx,2,1:m); (Adiabatic face) (11)

Conduction continuity at the interface SnO_2/SiO_2:

$$T^n(i,j) = \left(\lambda_{SiO2}\,T^n(i,j-1) + \lambda_{SnO2}\,T^n(i,j+1)\right)/\left(\lambda_{SiO2} + \lambda_{SnO2}\right)$$

Conduction continuity at the interface Si/SiO_2:

$$T^n(i,j) = \left(\lambda_{si}T^n(i,j-1) + \lambda_{SiO2}\,T^n(i,j+1)\right)/\left(\lambda_{Si} + \lambda_{SiO2}\right)$$

When there is porosity (air layer) between SnO_2 and SiO_2:

Conduction and convection continuities at the interface SnO_2/air:

$$\lambda_{SnO_2}\left(T^n(i,j+1) - T^n(i,j)\right)/Dy = \lambda_{air}\left(T^n(i,j) - T^n(i,j-1)\right)/Dy + h\left(T_a - T^n(i,j)\right)$$

Conduction & convection continuities at the interface air/SiO_2:

$$\lambda_{SiO2}\left(T^n(i,j) - T^n(i,j-1)\right)/Dy = \lambda_{air}\left(T^n(i,j+1) - T^n(i,j)\right)/Dy + h\left(T_a - T^n(i,j)\right)$$

Scheming with the finite element method

To solve the Equation (3) by the finite element method, the residue weighed in the Galerkin formulation as reported by Poulain et al. [14] and Hatta et al. [15] is used. The heat equation is multiplied by an arbitrary function T^*, called the weighing function, and integrated along the volume. Thus, the formulation of the integral of the low thermal problem is obtained:

$$w\left(T,T^*\right) = \int_V T^*\rho Cp\dot{T}dV + \int_{S\varphi} T^*h\left(T - T_a\right)dS + \int_V grad\left(T^*\right).\left(\lambda.grad\left(T\right)\right)dV = 0 \quad (12)$$

The analytical solution of equation (12) is generally inaccessible. The numerical solution by the finite element method, which is a particular case of the Galerkin method, (the temperature field and the test functions are belonging to the same finite-dimensional space), is used. The medium is divided into a finite number of elements interconnected only at nodal points. For each element occupying the space, the temperature at any point can be expressed as a function of their values to their nodal point:

$$T(x,y,t) = [N]\{T\} \quad (13)$$

Where [N] is known as a form of matrix and a function of spatial positions, {T} is a vector which contains the values of the temperature at the nodal points of the element. It follows that the temperature gradient at any point can be written as:

$$\{grad(T)\} = T\{\partial T/\partial x, \partial T/\partial y\} = [B]\{T\} \quad (14)$$

Where [B]=[L][N] and [L] designates a differential operator.

Substituting equation (14) in equation (3), the heat flux in the

element can be obtained as follows:

$$\{q\} = T\{q_1, q_2\} = -\lambda[B]\{T\} \quad (15)$$

Assume that the medium undergoes a virtual temperature change, δT. Then, multiplying Equation (12) by δT and by incorporating into the whole of the space domain, and with the substitution of the Equations (13) and (15), the finite element approximation of the heat equation, can be obtained by:

$$w(T, T^*) = \{T^*\}^T \left([D]\{\dot{T}\} + ([C]+[N])\{T\} - [M]\right) = 0 \quad (16)$$

Where, the dot represents differentiation, while respecting time. The elementary matrices and the vector of the external heat load are given by:

$$[D] = \int_V \rho C_p [N]^T [N] dV \quad (17)$$

$$[C] = \int_V [B]^T \lambda [B] dV \quad (18)$$

$$[N] = \int_{S\varphi} [N]^T h [N] dS \quad (19)$$

$$[M] = \int_{S\varphi} [N]^T h T_a dS \quad (20)$$

[D] is the thermal capacity matrix; [C] is the thermal conductivity matrix, [N] is the thermal convection matrix, and [M] is the nodal flux vector.

Using the finite difference scheme, Equation (16) becomes:

$$[D]\left(\{T\}^{n+1} - \{T\}^n\right)/\Delta t + ([C]+[N])\{T\}^n - [M] = 0 \quad (21)$$

Equation (21) is solved using an explicit finite difference method and Gauss-Legendre integration.

Results and Discussion

Numerical model validation

After both numerical models reach the calculation stability condition, comparisons (Figure 5) between the results for a sample of silicon coupled to silicon dioxide on the one hand, and a sample of silicon coupled to silicon dioxide, and tin dioxide, on the other hand, are performed. The results show satisfactory qualitative and quantitative agreements. Unlike in some profiles, comes from the numerical method (the finite difference method), which is considered less perfect than the finite element one.

Physical parameters influence on the thermal transfer phenomenon

In the following, the finite element method and the thermal conductivity of tin dioxide which has a parabolic profile relative to the temperature are used. This latter strongly influences on the heat transfer mechanisms of the system.

Effect of the imposed temperature: The study is carried out on heterojunction device $SnO_2/SiO_2/Si$, of different depths (0.2 μm/50 nm/1 μm), and a length of 1μm, with different temperatures applied to the surface of SnO_2.

It is noted that the initial temperature begins to increase along the depth of the sample, and a function of time, to reach the corresponding heating temperature. If the heat flux applied to the surface of SnO_2 increases, the minimum temperature will decrease. To better observe this phenomenon, the results in the form of linear temperature profiles are presented:

The curves of the Figure 6 show the evolution of the temperature during the heat transfer in the multilayer nanomaterials $SnO_2/SiO_2/Si$ that is subject only to the conduction. After 100ns, if the applied temperature increases, the applied heat flux also increases. Then, the profile of the thermal conductivity of SnO_2 can no longer withstand this temperature increase. According to Figure 6, if the applied temperature is between 300 K and 423 K, the temperature starts from 298.08 K and 384.23 K respectively, and increases with time to reach the heating temperature. But if the applied temperature is beyond 423 K, the system temperature breakdown and it remains at its initial temperature. In the following, the applied temperature of 423 K will be used.

Tin dioxide thickness effect: Similarly, the study is carried out on heterojunction device $SnO_2/SiO_2/Si$, where the depth of the SnO_2 is variable (x μm/50 nm/1 μm). The applied temperature is taken equal to 423K.

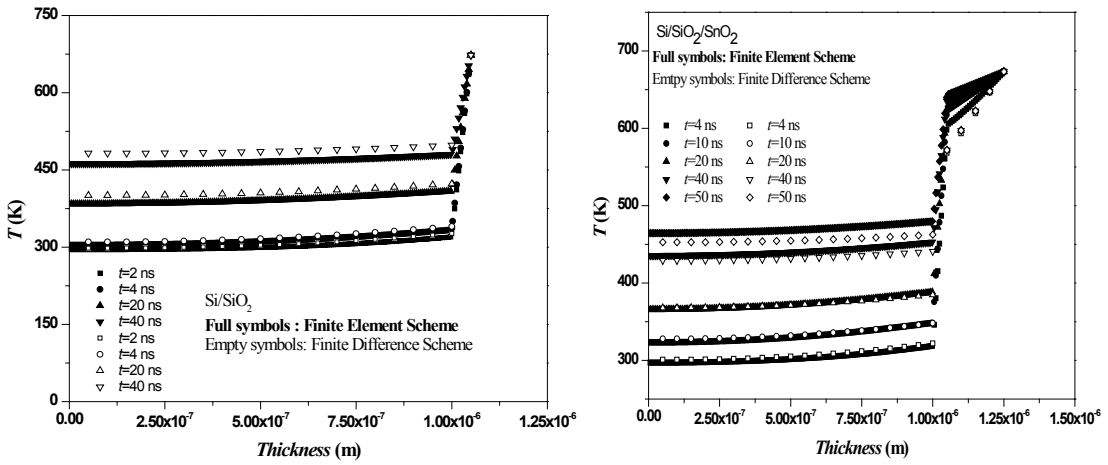

Figure 5: Comparison curves between both numerical methods.

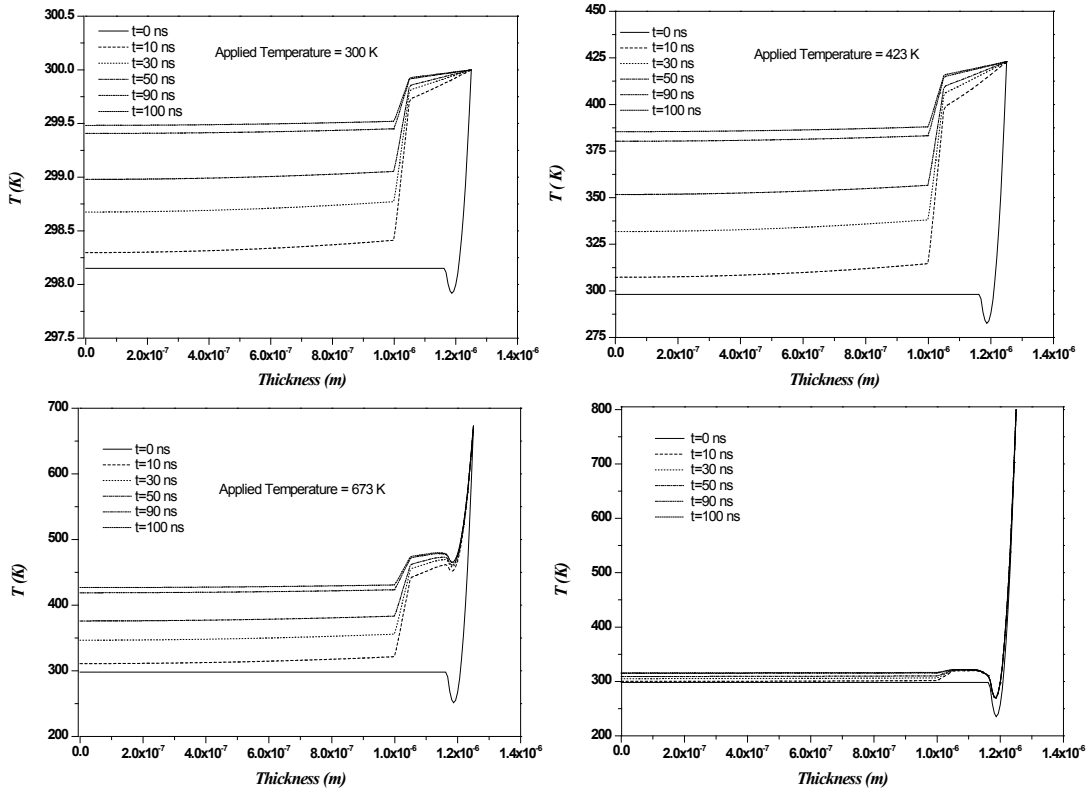

Figure 6: Axial evolution of the temperature in $SnO_2/SiO_2/Si$ for different applied temperatures.

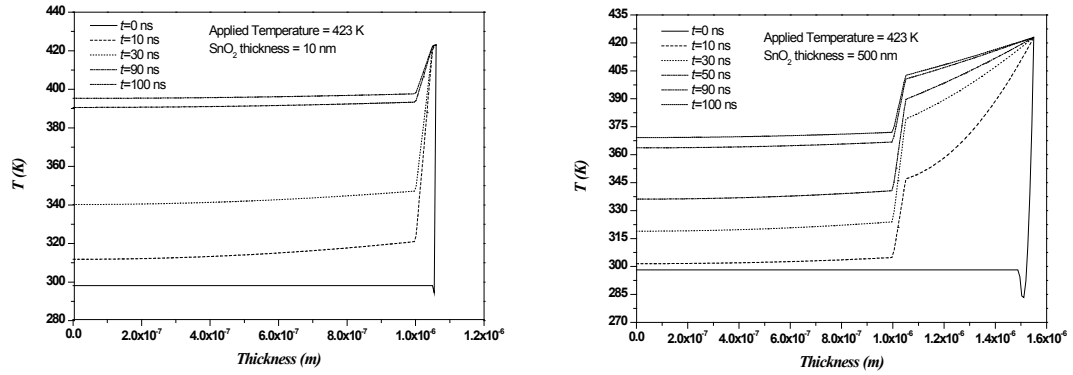

Figure 7: Axial evolution of the temperature in the $SnO_2/SiO_2/Si$ for different SnO_2 thicknesses.

It is noted that the initial temperature, begins to increase along the depth of the sample, and a function of time, in order to reach the heating temperature (423K). Quantitatively, if the thickness of the SnO_2 layer increases, the temperature profile will become less important because the thickness of the first layer (SnO_2) prevents heat easily diffuse into the depth of the sample, leading to the temperature decrease in the deeper layers. Qualitatively, if the thickness of the SnO_2 layer increases, the parabolic evolution of the temperature profile appears clearly. This evolution is deducted, from the impact of the parabolic profile of the thermal conductivity, on the heat transfer phenomenon, in the SnO_2 layer. It is noted that, in the case where the thermal conductivity is variable, the increase of the initial temperature to the heating one is less than in the case where the thermal conductivity is constant. Figure 7 represents the temperature linear profiles:

These curves show the evolution of the temperature during the heat transfer into the multilayer $SnO_2/SiO_2/Si$, which is subject only to the conduction. During 100ns, the heterojunction device will heat up more quickly if the thickness of SnO_2 is less than 0.2 μm. If the thickness of SnO_2 is 10 nm and for a time of 100 ns, the temperature increases from its initial value of 395.3 K to reach its hot value (423 K). But, for a thickness of SnO_2, above 0.2 μm (e.g., 500 nm), and a time of 100 ns, the temperature increases from 369.191 K, to reach its heating temperature (423 K). Therefore, the decrease of the initial value of the temperature

in the deep layer of the sample is particularly important, if the thickness of the tin dioxide layer is large. Then, to exhaust heat through the depth of the sample, it is better to choose a thickness of the thin films of tin dioxide lower than 0.2 µm.

Porosity effect on the heat transfer: The effect of the porosity on the heat transfer in the heterojunction device is studied numerically. Porosity is an air layer defined by the two layers of SnO_2 and SiO_2. The thermal analysis is performed on the sample SnO_2/Air/SiO_2/Si in the form of a sandwich. A heating temperature, equal to 423K, is applied to the surface of SnO_2. The dimensions and the thermal conductivities of the various layers are presented in the following Table 1.

Similarly, the results are presented as temperature profiles, as the following Figure 8.

These curves show the evolution of the temperature during the heat transfer in the SnO_2/Air/SiO_2/Si, taking account of the conduction and convection, to interfaces SnO_2/Air and Air/SiO_2. The presence of the air layer (porosity) coming from a deposition problem of a semiconductor thin layer on a substrate prevents the temperature of the latter to evacuate quickly. This kind of transfer leads to a rapid temperature increase in the semiconductor layer. The three presentations of Figure 8 show the existence of two levels. The first level corresponds to the heating of the SnO_2 layer, and the second one corresponds to the heating of the Si/SiO_2 layer. Unfortunately, the intermediate portion between the two levels insulates thermally, the semiconductor of the substrate, and prevents the semiconductor temperature to evacuate quickly [16-19].

Materials	Dimensions	Thermal Conductivities
SnO_2	1 µm*0.2 µm	$-2.136 \times 10^{-4} \times T^2+0.078 \times T+27.484$ W/ (m.K)
SiO_2	1 µm*50 nm	1.4 W/(m.K)
Si	1 µm*1 µm	149 W/(m.K)
Air	1 µm*25 nm	$3.7 \times 10^{-4}+T(9.32 \times 10^{-5}-2.59 \times 10^{-8} \times T)$

Table 1: Dimensions and thermal conductivities of SnO_2/Air/SiO_2/Si.

Figure 9 indicates clearly the difference between the sample of SnO_2/Air/SiO_2/Si and that of SnO_2/SiO_2/Si. The difference between the two curves is becoming more important with time. This difference is due to the presence of porosity. It traps the temperature in the SnO_2 layer. For a time t=100 ns remarkable jump between the two curves is presented. Then, the presence of the porosity between the thin layer and the substrate highly insulates the top of the sample (thin layer) and entraps the temperature in the latter; this reduces the heat transfer phenomenon from the top to the bottom of the sample.

Conclusion

The two-dimensional heat transfer equation, that is coupled to the initial and boundary conditions at different interfaces of heterojunction device (SnO_2/SiO_2/Si) and/or (SnO_2/Air/SiO_2/Si), taking into account the variability of the thermal conductivity of the tin dioxide, is studied numerically. If the contact between the tin dioxide layer and the substrate is made without the presence of a porosity (air layer), the

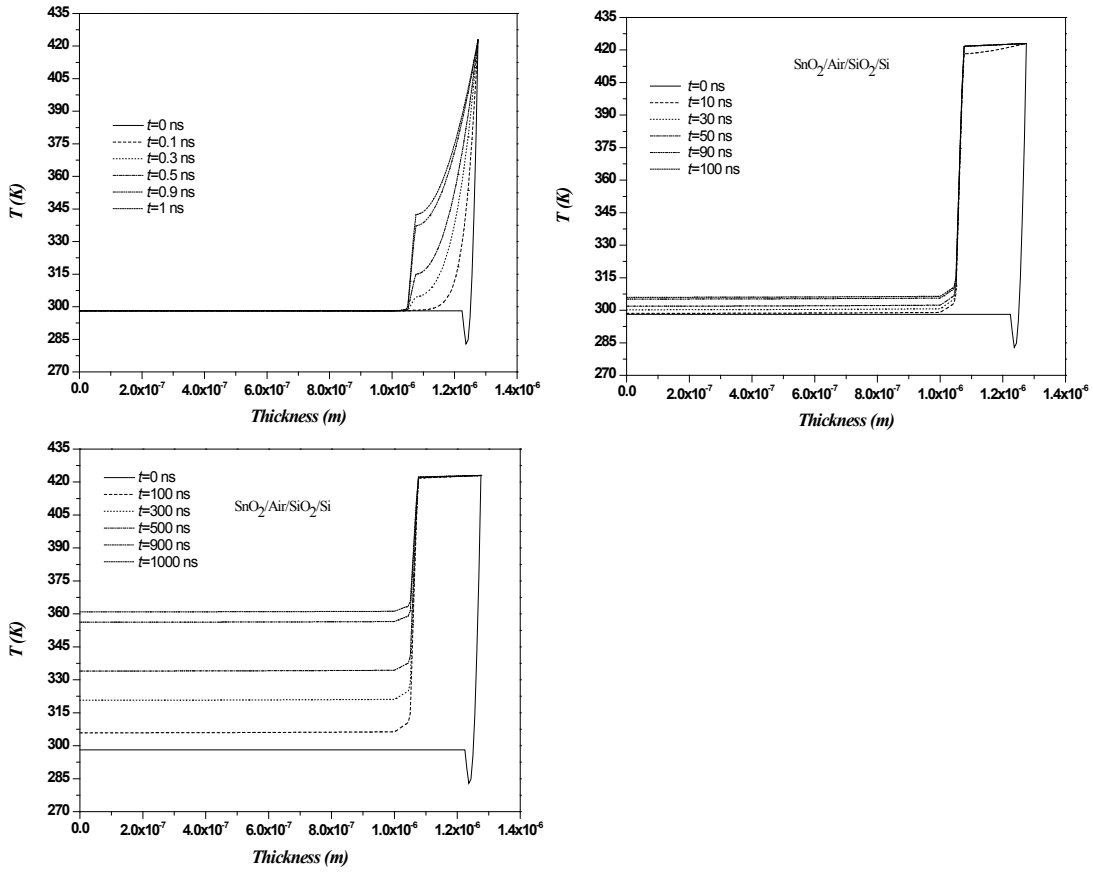

Figure 8: Axial evolution of the temperature in SnO_2/Air/SiO_2/Si in 1,100 and 1000 ns.

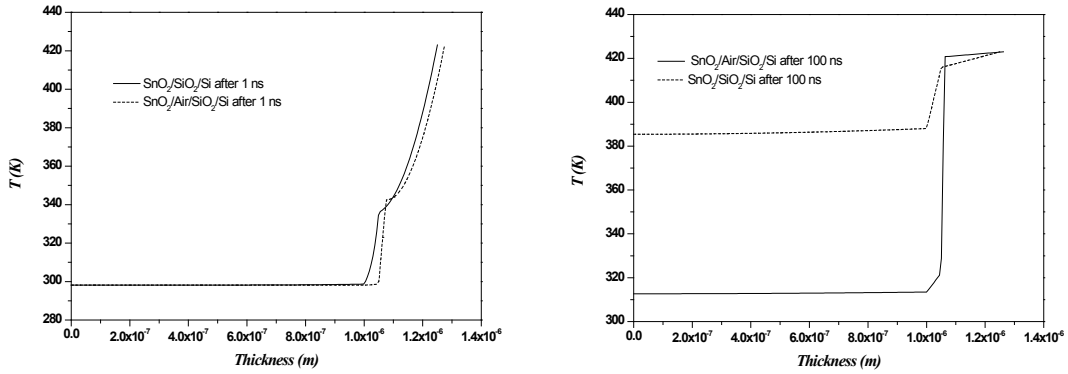

Figure 9: Comparison between the two sandwiches SnO_2/Air/SiO_2/Si and SnO_2/SiO_2/Si.

coupling is done by the continuity of the conduction at the interfaces. Otherwise, the coupling is realized by the continuity of the conduction and convection at the interfaces. The mathematical model is schemed by two different methods: the explicit finite difference method and the finite element method. The results are the following:

1. Comparison between both results of the two numerical methods showed satisfactory qualitative and quantitative agreements to both Si/SiO_2 and Si/SiO_2/SnO_2, and that the results of the finite element method is more efficient than that of the finite difference ones.

2. The results of the finite element method show that the variable thermal conductivity of tin dioxide does not permit to apply a high thermal gradient between the surface of the sample and the other layers, which prevents to apply a temperature higher than 423 K.

3. The influence of layer thickness of tin dioxide on the heat transfer through the heterojunction device is studied. Therefore, the decrease of the initial value of the temperature in the deep layer of the sample is particularly important, if the thickness of the SnO_2 layer is large. Then, to exhaust heat through the depth of the sample, it is better to choose a thickness of the thin films of tin dioxide lower than 0.2 μm.

4. Finally, during the deposition of the thin layer, the presence of the porosity (air layer) between the thin layer and the substrate highly insulates the top of the sample (tin dioxide layer) and entraps the temperature in the latter; this reduces the heat transfer phenomenon from the top to the bottom of the sample. Thus, a thermal fatigue can contribute an electrical strain which decreases the electrical efficiency of the system.

Acknowledgement

This work is supported by the doctorate school of sciences and technologies of the Lebanese University, EDST-UL.

References

1. Baoding L (2002) Theory and Practice of Uncertain Programming (1st Eds.). Physica-Verlag, Heidelberg.
2. Feng L, Li T, Ruan D, Gou S (2011) A vague-rough set approach for uncertain knowledge acquisition. Knowledge-Based Systems 24: 837-843.
3. Osman MS, Lashein EF, Youness EA, Atteya TEM (2011) Mathematical Programming in Rough Environment. Optimization: A Journal of Mathematical Programming and Operations Research 60(5): 603-611.
4. Youness EA (2006) Characterizing solutions of rough programming problems. European Journal of Operational Research 168(3): 1019-1029.
5. Pawlak Z (1982) Rough sets. International Journal of Computer and Information Sciences 5: 341-356.
6. Pawlak Z (1991) Rough Sets-Theoretical Aspects of Reasoning about Data. Kluwer Academic Publishers, Boston.
7. Pawlak Z (1996) Rough Sets, Rough Relations and Rough Functions. Fundamental Inform 27(2/3): 103-108.
8. Pawlak Z (1997) Vagueness-A rough set view. Structures in Logic and Computer Science, Springer: 106-117.
9. Pawlak Z (2002) Rough set theory and its applications. Journal of Telecommunications and information technology.
10. Abu-Donia HM (2012) Multi Knowledge based rough approximations and applications. Knowledge Based Systems 26: 20-29.
11. Tao Z, Xu J (2012) A class of rough multiple objective programming and its application to solid transportation problem. Information Sciences 188: 215-235.
12. Xu J, Yao L (2009) A class of multiobjective linear programming models with random rough coefficients. Mathematical and Computer Modelling 49: 189-206.
13. Chankong V, Hiams YY (1983) Multiobjective decision making: Theory and methodology. North Holland, New York.
14. Li ZF, Wang SY (1994) Lagrange multipliers and saddle point in multiobjective programming. Journal of optimization theory and application 83(1): 63-81.
15. Tanino T, Sawaragi Y (1979) Duality theory in multiobjective programming. Journal of optimization theory and application: 27(4).
16. Yan Z, Li S (2004) Saddle point and generalized convex duality for multiobjective programming. Appl computing 15(1-2): 227-235.
17. Bazaraa MS, Sherali H, Shetty CM (2006) Nonlinear Programming - Theory and Algorithms (3rd Eds.). Wiley-Inter science.
18. Osman MSA (1977) Qualitative analysis of basic notions in parametric convex programming I. Applications of Mathematics 22(5): 318-332.
19. Osman MSA (1977) Qualitative analysis of basic notions in parametric convex programming II. Applications of Mathematics 22(5): 333-348.